

Evaluation of the liver function by the liver parenchyma, spleen and portal vein signal intensity during the hepatobiliary phase in Gd-EOB-DTPA-enhanced MRI

Ming Yang

Second Affiliated Hospital of Soochow University

Yue Zhang

Second Affiliated Hospital of Soochow University

Wenlu Zhao

Second Affiliated Hospital of Soochow University

Wen Cheng

Second Affiliated Hospital of Soochow University

Han Wang

Second Affiliated Hospital of Soochow University

Shengren Guo (✉ Guosrsdefy@163.com)

Second Affiliated Hospital of Soochow University <https://orcid.org/0000-0002-8935-9954>

Research article

Keywords: Gd-EOB-DTPA, Magnetic resonance imaging, Liver function, Portal vein, Spleen

Posted Date: August 22nd, 2020

DOI: <https://doi.org/10.21203/rs.3.rs-17044/v2>

License:  This work is licensed under a Creative Commons Attribution 4.0 International License.

[Read Full License](#)

Version of Record: A version of this preprint was published on October 20th, 2020. See the published version at <https://doi.org/10.1186/s12880-020-00519-7>.

Abstract

Background: Previous studies used the signal intensity (SI) to reflect liver function. However, there are still few studies on the assessment of liver function via the portal vein, and no study has pointed out that in terms of SI (liver, spleen, portal vein), which one can better reflect liver function. Therefore, the aim of this study is to investigate whether these parameters can be used to evaluate liver function in patients with cirrhosis and determine which parameter is best.

Methods: A total of 120 patients with normal livers ($n = 41$) or Child–Pugh class A ($n = 50$), B ($n = 21$) or C ($n = 8$) disease who underwent Gd-EOB-DTPA-enhanced MRI were retrospectively reviewed. Comparisons of the SI of the liver parenchyma, portal vein, and spleen and liver-to-portal vein (LPC), liver-to-spleen (LSC), and portal vein-to-spleen (PSC) contrast ratios on the 15-min hepatobiliary phase images were performed among groups, and the correlations among liver function parameters (total bilirubin, direct bilirubin, indirect bilirubin, aspartate aminotransferase, alanine aminotransferase, albumin, creatinine, platelet count, prothrombin time and international normalized ratio), liver function scores and MRI date were also quantitatively analyzed.

Results: Significant differences were observed in the SI of the liver parenchyma, LPC and LSC among groups. These values all decreased gradually from normal livers to Child–Pugh class C cirrhotic livers ($P < 0.001$). The SI of the portal vein constantly and slightly increased from normal livers to Child–Pugh class C cirrhotic livers, but there were no differences among groups in portal vein signal and PSC ($P > 0.05$). LPC had a stronger correlation with Child-Pugh score and MELD score than LSC and liver parenchyma SI. The order of the AUCs of these parameters, from largest to smallest, was as follows: LPC, LSC, and liver parenchyma SI ($P > 0.05$).

Conclusion: Liver parenchyma SI, LSC and LPC may be used as alternative imaging biomarkers for assessing liver function, while the portal vein signal and PSC could not reflect liver function. Furthermore, LPC values can more effectively distinguish severity among patients with cirrhosis than liver parenchyma SI and LSC.

Background

The assessment of liver function is one of the most important issues in patients with cirrhosis. The Child-Pugh score and model for end-stage liver disease (MELD) score are commonly used in clinical work. However, these scores all have some design flaws. The five indicators (total bilirubin (TB), albumin, creatinine, prothrombin time (PT), ascites and hepatic encephalopathy) in the Child-Pugh score have no weight distinctions, and each indicator is greatly affected by other factors. The judgment of ascites and hepatic encephalopathy is subjective. The MELD score includes three indicators (TB, creatinine and international normalized ratio (INR)), which can overcome the influence of subjective factors. However, this score does not consider portal hypertension and complications, and some nonliver disease factors

may also affect TB, INR, and creatinine levels. In addition, both scores are only used to evaluate whole liver function.

Gadolinium-ethoxybenzyl-diethylenetriamine penta-acetic acid (Gd-EOB-DTPA) is a kind of hepatocellular contrast agent. It is easily taken up by normal hepatocytes and secreted into the biliary system without any change in its chemical structure [1]. Additionally, Gd-EOB-DTPA has characteristics of both nonspecific extracellular space contrast agents and hepatocyte-specific contrast agents [2]. Therefore, Gd-EOB-DTPA-enhanced MR imaging has been used not only for the detection and characterization of liver lesions [3-6] but also for a one-stop assessment of hepatic function. Compared with the above two scoring systems, the greatest advantage of using MRI to evaluate liver function is that this method has great potential for evaluating liver function at and below the liver segment. In addition to functional information, the data required for surgical planning, such as tumor volume and distribution, liver anatomy, vascular supply, and related extrahepatic findings, can also be collected in one examination. Thus, it is possible to accurately predict the effective residual liver function after the operation and guide clinicians in adopting appropriate treatment plans for patients.

Previous studies have evaluated liver function through Gd-EOB-DTPA-enhanced MRI, including biliary tract enhancement [7], the liver signal intensity ratio with or without reference groups [8], T1 mapping [9], and dynamic contrast-enhanced MR imaging [10]. However, using the signal intensity ratio to assess liver function is the simplest and most convenient method. The relative enhancement ratio (RE) of the liver parenchyma and liver-to-spleen contrast ratio (LSC) have been widely described [11-13]. However, there are still few studies on the assessment of liver function via the portal vein, and no study has pointed out that in terms of these parameters (SI of the liver parenchyma, portal vein, and spleen and liver-to-portal vein (LPC), liver-to-spleen (LSC), portal vein-to-spleen (PSC) contrast ratios), which one can better reflect liver function. Therefore, the aim of this study is to investigate whether these parameters can be used to evaluate liver function in patients with cirrhosis and determine which parameter is best.

Methods

Patients

This retrospective study of existing data was approved by the institutional review board, and the requirement for written informed consent was waived.

In the period from November 2017 to October 2019, 761 Gd-EOB-DTPA-enhanced MR imaging examinations were performed. The exclusion criteria were as follows: liver function tests were not performed within 1 week before and after MR examination (n = 288); excessive motion artifacts or incomplete examination (n = 36); the main portal vein and its right and left branches were not visualized on MR images, typically because of thrombosis or tumor thrombosis (n = 33); splenectomy or diffuse Gamna-Gandy bodies (n = 11); presence of diffuse or massive (d > 10 cm) liver tumor, hemangiomas, cysts and partial hepatectomy (n = 76); liver dysfunction without cirrhosis (n = 88); and various diseases of the biliary tract such as cholelithiasis or biliary duct dilatation and kidney failure (n = 109). In total, 120

patients with the following diagnoses were included in our retrospective study: HBV-related cirrhosis (n = 52), HCV-related cirrhosis (n = 13), alcoholic cirrhosis (n = 5), and schistosomal cirrhosis (n = 9).

Clinical data

Two radiologists separately recorded the clinical data of the patients, including age, sex, biochemical tests associated with liver function (TB, direct bilirubin, indirect bilirubin, aspartate aminotransferase (AST), alanine aminotransferase (ALT), albumin, creatinine, platelet count, prothrombin time (PT), INR) and clinical manifestations (ascites, hepatic encephalopathy) and also obtained the Child-Pugh score and MELD score. For all patients, Roche Cobas 8000 automatic chemistry analysis was used for biochemical tests. The two radiologists reviewed the records and reached an agreement. To ensure that the MELD score was positive, we noted TB and INR values as 1.00 when their values were less than 1.00.

MR imaging technique

All examinations were performed on a 3.0 T magnetic resonance system (Ingenia 3.0 T, Philips, Netherlands) using a 32-channel phased-array coil. Enhanced scanning was performed using a modified Dixon (mDixon) sequence. The parameters for mDixon were as follows: repetition time, 3.79 ms; echo time, 1.33 ms; sense factor, 2.0; flip angle, 18°; field of view, 352 × 400 mm; matrix, 268 × 236; reconstruction matrix, 400 × 400; bandwidth, 1260.6 Hz per pixel; scan time, 15 s; and thickness, 5 mm. The HBP images were obtained 15 min after Gd-EOB-DTPA administration. Gd-EOB-DTPA (Primovist; Bayer Schering Pharma AG, Berlin, Germany) was used as a hepatocellular contrast agent. All patients received the contrast agent injection at a rate of 1.0 mL/s (dose = 0.025 mmol/kg body weight). The contrast agent was intravenously administered via a power injector followed by a 25.0 mL saline flush.

Imaging analysis

All examinations were reviewed by two other radiologists with 3 and 10 years of experience in abdominal MR imaging who were blinded to the patients' clinical, laboratory, and radiological information. Regions of interest (ROIs) were applied to the liver and spleen parenchyma and main, right, and left portal veins on the 15-min HBP images in a picture archiving and communication system (PACS; Neusoft, Shenyang, China). Each ROI was either a circle or an oval. The SI of the liver parenchyma was measured in four sections (left lateral, left medial, right anterior, and right posterior). The SI of the spleen parenchyma was measured in three evenly distributed sections. In each section of the liver and spleen, the ROI (ROI size: 200 mm²) was manually set by the observers, avoiding visible vessels and biliary ducts, focal lesions, and imaging artifacts. The portal vein ROIs were separately placed in the center of the main portal and its right and left branches based on the location of the vessels in the portal phase. The size of each ROI depended on the diameter of the portal vein (ROI size: 8-40 mm²). LPC was calculated by dividing the liver parenchyma SI by the portal vein SI, LSC was calculated by dividing the liver parenchyma SI by the spleen SI, and PSC was calculated by dividing portal vein SI by the spleen SI on the 15-min HBP images as follows:

$$\text{LPC} = [\text{SI}_{\text{liver}}]/[\text{SI}_{\text{Portal vein}}]$$

$$\text{LSC} = [\text{SI}_{\text{liver}}]/[\text{SI}_{\text{spleen}}]$$

$$\text{PSC} = [\text{SI}_{\text{Portal vein}}]/[\text{SI}_{\text{spleen}}]$$

Statistical analysis

Statistical analysis was performed with IBM SPSS Statistics (version 25.0, Chicago, IL). The Kolmogorov-Smirnov test was used to evaluate the normality of the measurement data. Normally distributed data are presented as the mean \pm standard deviation, and nonnormally distributed data are presented as the median (interquartile range). One-way ANOVA or the nonparametric Kruskal–Wallis test was used to compare the differences between the normal group and Child–Pugh class A, B, and C groups. One-way ANOVA with LSD or the rank sum test with the Mann-Whitney U test was applied for analyses among groups. Spearman rank correlation coefficients were used to analyze the correlation between hepatic function laboratory markers and MRI data of the 15-min HBP images. ROC analysis was used to discriminate between group 1 (normal group and Child–Pugh class A) and group 2 (Child–Pugh class B and C) on the 15-min HBP images. All tests were two-sided, and a $p < 0.05$ indicated statistical significance.

Results

Clinical data and laboratory examination

All 120 subjects included normal patients ($n = 41$), and Child–Pugh class A ($n = 50$), B ($n = 21$) and C ($n = 8$). Laboratory parameters and clinical data of patients are shown in Table 1. There were no significant differences in the age, gender, creatinine and mean interval (between MRI and laboratory testing) among the groups. However, distinct differences were identified in all analyzed groups regarding TB, albumin, ALT, AST, PLT, PT, INR, Child–Pugh score, and MELD score ($P < 0.001$).

Table 1
Laboratory texts and clinical information of the patients.

Characteristic	Total	Normal	C-P A	C-P B	C-P C	P value
Sample size	n = 120	n = 41	n = 50	n = 21	n = 8	-
Child-Pugh score	6.0 (5.0-7.0)	-	5.0 (5.0-6.0)	7.0 (7.0-8.0)	12.0 (11.3-12.0)	< 0.001
MELD score ^a	7.41 (6.43-8.52)	6.43 (6.43-6.43)	7.50 (7.12-7.97)	10.04 (8.55-10.50)	16.33 (15.34-16.69)	< 0.001
Mean interval(days) ^a	2.0 (0.3-4)	2.0 (1.0-4.0)	1.0 (0.0-3.3)	2.0 (0.5-3.0)	3.0 (1.3-5.0)	0.177
Age (years) ^a	56.0 (52.0-64.8)	54.0 (49.5-58.5)	60.0 (52.0-64.3)	60.0 (52.5-66.5)	55.0 (45.3-71.5)	0.208
Gender(male/female)	73 / 47	25 / 16	32 / 18	13 / 8	3 / 5	0.566
Standard hepatic function test						
TB (mg/dL) ^a	0.85 (0.60-1.18)	0.54 (0.40-0.65)	0.92 (0.80-1.09)	1.35 (1.13-1.88)	3.45 (3.13-3.95)	< 0.001
Albumin (g/dL) ^a	4.28 (3.90-4.57)	4.60 (4.41-4.71)	4.20 (4.10-4.40)	3.50 (2.96-3.82)	2.61 (2.39-2.64)	< 0.001
INR ^a	1.07 (0.99-1.15)	0.96 (0.95-1.00)	1.09 (1.05-1.12)	1.19 (1.15-1.24)	1.53 (1.47-1.67)	< 0.001
PT ^a	13.9 (12.8-14.6)	12.5 (12.3-12.8)	14.1 (13.8-14.5)	14.9 (14.4-15.8)	18.6 (18.1-19.2)	< 0.001
Serum hepatic enzyme levels						
AST (U/L) ^a	26.0 (18.0-38.0)	17.0 (14.0-21.0)	29.0 (21.0-37.3)	40.0 (34.5-61.0)	87.0 (70.3-92.8)	< 0.001
ALT (U/L) ^a	25.0 (17.0-35.8)	17.0 (11.5-21.0)	27.0 (21.0-37.3)	39.0 (34.0-42.5)	71.0 (63.3-84.3)	< 0.001
MELD, model for end-stage liver disease; TB, total bilirubin; INR, international normalized ratio; PT, Prothrombin time; AST, aspartate transaminase; ALT, alanine transaminase.						
^a For the quantitative analysis, the non-normal distribution data is presented as median (interquartile range).						

Characteristic	Total	Normal	C-P A	C-P B	C-P C	P value
Serum renal function levels						
Creatinine (mg/dL) ^a	0.73 (0.67– 0.82)	0.71 (0.65– 0.77)	0.76 (0.69– 0.90)	0.72 (0.64– 0.78)	0.76 (0.70– 0.95)	0.132
Platelet count ^a	135 (81.0– 209.8)	230.0 (182.0– 262.0)	124.5 (84.8– 143.0)	78.0 (68.5– 90.0)	48.5 (36.8– 66.8)	< 0.001
MELD, model for end-stage liver disease; TB, total bilirubin; INR, international normalized ratio; PT, Prothrombin time; AST, aspartate transaminase; ALT, alanine transaminase.						
^a For the quantitative analysis, the non-normal distribution data is presented as median (interquartile range).						

Differences of MRI data among groups at HBP 15 min

Liver parenchyma SI, LPC and LSC values were significantly different in all groups at HBP 15 min ($p < 0.001$), and they gradually decreased from normal to Child–Pugh C cirrhotic livers. Spleen parenchyma SI, portal vein SI and PSC values were not significantly different in all groups, and portal vein SI constantly and slightly increased from normal to Child–Pugh class C ($p > 0.05$), as shown in Table 2. Hepatobiliary phase images among the groups are shown in Fig. 1.

Table 2
Differences of MRI data among groups at HBP 15 min

	Total	Normal	C-P A	C-P B	C-P C	P value
SI _{liver} ^a	459.2 ± 112.5	528.1 ± 100.3	458.9 ± 98.1	383.7 ± 71.2	312.6 ± 64.5	< 0.001 ^b
SI _{spleen} ^a	284.7 ± 70.6	279.1 ± 75.1	279.3 ± 73.6	305.8 ± 58.3	296.3 ± 55.7	0.794
SI _{portal vein} ^a	268.3 ± 80.9	254.1 ± 80.9	258.3 ± 79.6	275.5 ± 76.7	298.7 ± 79.3	0.626
LPC ^a	1.80 ± 0.58	2.17 ± 0.50	1.86 ± 0.63	1.34 ± 0.47	0.96 ± 0.13	< 0.001 ^c
LSC ^a	1.67 ± 0.47	1.98 ± 0.43	1.69 ± 0.34	1.29 ± 0.32	0.93 ± 0.16	< 0.001 ^d
PSC ^a	0.93 ± 0.14	0.93 ± 0.13	0.92 ± 0.12	0.95 ± 0.15	0.99 ± 0.19	0.213
^a The normal distribution data is presented as mean ± standard deviation.						
^b The statistical difference was found in SI _{liver} at HBP 15 min among all groups (p < 0.001) except C-P B and C-P C (p = 0.023).						
^c The statistical difference was found in LPC at HBP 15 min among all groups (p < 0.001) except C-P B and C-P C (p = 0.047).						
^d The statistical difference was found in LSC at HBP 15 min among all groups (p < 0.001) except C-P B and C-P C (p = 0.020).						

The correlation between laboratory markers and MRI data at hepatobiliary phase 15 min

The correlations between laboratory markers and MRI data at HBP 15 min are summarized in Table 3. TB, albumin, PT, INR, PLT, ALT, AST, Child-Pugh score, and MELD score were significantly correlated with liver parenchyma SI, LPC and LSC. And there a strong correlation was observed between LPC and LSC with respect to all groups, as you can see in Fig. 2.

Table 3

The correlation among clinical parameters, LPC or LSC in cirrhosis groups at hepatobiliary phase 15 min.

Laboratory indexes	Correlation coefficient			P value
	LPC	LSC	SI _{liver}	
TB	-0.577	-0.613	-0.522	< 0.001
Albumin	0.565	0.623	0.479	< 0.001
ALT	-0.426	-0.455	-0.492	< 0.001
AST	-0.477	-0.512	-0.506	< 0.001
INR	-0.641	-0.646	-0.553	< 0.001
PT	-0.579	-0.576	-0.524	< 0.001
Creatinine	-0.090	-0.139	0.024	> 0.050
Platelet count	0.464	0.467	0.518	< 0.001
Child-Pugh score	-0.576	-0.569	-0.562	< 0.001
MELD score	-0.632	-0.580	-0.526	< 0.001

TB, total bilirubin; ALT, alanine transaminase; AST, aspartate transaminase; INR, international normalized ratio; PT, Prothrombin time; MELD, model for end-stage liver disease.

ROC analysis

The ROC curve analysis revealed the optimal cutoff value for LPC to distinguish group 1 (normal group and Child–Pugh class A) from group 2 (Child–Pugh class B and C) was 1.20 (AUC 0.892) with a sensitivity of 98.9% and a specificity of 69.0%. The optimal cutoff value for LSC to distinguish group 1 from group 2 was 1.27 (AUC 0.889) with a sensitivity of 95.6% and a specificity of 72.4%. The optimal cutoff value for liver parenchyma SI to distinguish group 1 from group 2 was 405.4 (AUC 0.836) with a sensitivity of 81.3% and a specificity of 75.9%. (Fig. 3). The differences of AUCs among LPC, LSC and the liver parenchyma SI were not significant ($p > 0.05$). The reason for this grouping was due to the cirrhosis patients with Child–Pugh class B or C contraindications for operation studies [17, 18].

Discussion

Cirrhosis can damage liver cells, increase spleen volume, and lead to portal hypertension, so we mainly assessed the liver, spleen and portal vein. Our research was conducted with 15-min HBP images, and we believed that this time period could meet the needs for diagnosing liver diseases and shorten the examination time of patients.

The liver parenchyma SI can be used to estimate liver function, which has been widely described. The hepatobiliary phase of Gd-EOB-DTPA-enhanced images is due to the selective uptake of membrane-bound organic anion transporters (OATP1 B1/B3) [16-18]. Normal hepatocytes can use these transporters to uptake Gd-EOB-DTPA, and the amount of Gd-EOB-DTPA peaked on the 20-min HBP images; the number of impaired transporters and functional capacity of these transporters could reduce the uptake of Gd-EOB-DTPA into hepatocytes [19], subsequently affecting the liver signal. Our data showed that liver parenchyma SI gradually decreases with increasing liver function damage. Previous studies [19-21] have also indicated that the severity of cirrhosis can significantly affect the absorption of gadolinium and then affect the degree of liver enhancement, which was consistent with our research.

The spleen does not contain the organic anion transporters described above, and Gd-EOB-DTPA only shows the characteristics of a nonspecific extracellular space contrast agent. Our research indicates that the SI of the spleen cannot reflect liver function, and the mean value of the spleen signal is equally likely in each group. In addition, we found that in most of the cases in this study, the spleen signal increased gradually from right to left on both pre-enhanced images or 15-min HBP images (Fig. 4), leading to an increase in the mean signal value of the spleen. The reason behind this phenomenon remains unclear and may be related to the uneven magnetic field or the hemodynamics of the spleen.

In our study, the portal vein SI constantly and slightly increased from the normal liver to Child–Pugh class C cirrhotic liver, but there were no differences among groups. Zhang reported that the LPC can effectively indicate the severity of liver function [22], and their data on portal vein SI are similar to our research. A previous study suggested that the delayed hyperintensity in the portal vein can potentially be used to reflect hepatobiliary function [23], the subjects in that study were mostly patients with extrahepatic cholestasis. There was no delayed hyperintensity in the portal vein in any of the subjects in this study, and the direct bilirubin levels in all groups were lower than the cut-off value of 2.18 mg/dl, except for one patient in group C (2.38 mg/dl). We think that is the main reason for the difference between studies. Hepatobiliary phase images among the groups are shown in Fig. 5. A study proved that hepatic uptake and biliary elimination of bilirubin compete against Gd-EOB-DTPA uptake, and hyperbilirubinemia will lead to decreased absorption and clearance of Gd-EOB-DTPA, which can also lead to delayed contrast agent clearance from the blood [24]. However, we hold that the bilirubin level in patients with cirrhosis may not be as high as that in patients with extrahepatic cholestasis, and hepatocytes may be able to withstand this competition in patients with cirrhosis.

Unlike that of enhanced CT, the signal intensity of enhanced MRI has a nonlinear relationship with the concentration of contrast agent, and most studies have used a reference tissue (spleen) to correct the liver signal. As we have seen, only one study has examined the relationship between LPC and LSC [25]. Their results showed that LPC was strongly correlated with LSC, and the LPC of each group was lower than the LSC. The authors believed that this was due to the portal vein SI, which can more reflect the blood pool than the spleen. Our research also showed a strong correlation between LPC and LSC among groups, but the LPC was greater than the LSC. The reasons for this difference may be as follows: (1) the different underlying causes might lead to the different patterns of uptake and excretion of Gd-EOB-DTPA

since our patients mainly had hepatitis B cirrhosis, and their patients mainly had chronic liver disease; and (2) the MRI devices and imaging sequences were different.

To the best of our knowledge, no one has studied PSC yet, and our research proved for the first time that PSC cannot reflect liver function in patients with cirrhosis. As discussed before, the portal vein SI consistently and slightly increased from normal liver to Child–Pugh class C cirrhotic liver, but there were no differences among groups, and the mean value of the spleen signals was likely equal across groups. It is possible that there is no difference in PSC among groups.

Some studies have used ICG to reflect liver function because there is a direct correlation between ICG clearance and hepatocytes, and this parameter can provide more complete information on liver uptake and excretion function [26-28]. We did not analyze ICG because of operational difficulties. We quantitatively analyzed the correlations between MRI data and liver function parameters. In this study, the liver parenchyma SI, LPC and LSC were weakly to moderately correlated with laboratory markers. Zhang also demonstrated a weak to moderate correlation between LPC and laboratory markers [22], which was consistent with our research. We also found that the liver parenchyma SI, LPC and LSC were negatively correlated with hepatic function scores (Child–Pugh score and MELD score), and the correlation coefficients of the parameters, in order from largest to smallest, was as follows: LPC, LSC, and the liver parenchyma SI. The reason may be that the changing trend of the portal vein signal strengthens the correlation between LPC and liver function.

Receiver operating characteristic analysis showed that the order of the AUCs of the parameters, from largest to smallest, was as follows: LPC, LSC, and the liver parenchyma SI (0.892, 0.889, 0.836); however, the differences in AUCs among LPC, LSC and the liver parenchyma SI were not significant. This illustrated that these parameters have the same ability to distinguish between group 1 and group 2.

These results suggested that LPC might be a more useful alternative imaging biomarker for evaluating liver function than LSC and the liver parenchyma SI. Takatsu found that LPC could be used as a substitute for LSC for a simple assessment of the degree of hepatic contrast enhancement [25], which is consistent with our research. In addition, the authors also believed that LPC can be especially useful in cases of splenectomy and Gamna–Gandy bodies [25]. However, we thought this conclusion needed further verification because of the small number of patients who underwent splenectomy ($n = 6$) and those with Gamna–Gandy bodies ($n = 7$), and these patients were Child–Pugh class B.

In addition, nuclear medicine tracers that assess liver function have also been reported, mainly ^{99m}Tc -galactosyl human serum albumin (GSA) and ^{99m}Tc -mebrofenin. GSA is an asialoglycoprotein analog, and mebrofenin is an iminodiacetic acid (IDA) analog [29]. The tracers ^{99m}Tc -GSA and ^{99m}Tc -mebrofenin can be specifically absorbed by hepatocytes after being injected into the body. The combination of SPECT and CT allows for 3D distribution analysis and more exact measurements. Therefore, these tracers can be used to accurately and quantitatively analyze the liver function reserve of each liver segment. However, the disadvantages are obvious, such as the fusion method of SPECT image and CT

image has not been standardized, radiation exposure and low image resolution. Rassam et al. compared dynamic gadoxetate-enhanced MRI and ^{99m}Tc -mebrofenin hepatobiliary scintigraphy with SPECT for the assessment of liver function and found that the mebrofenin uptake rate (MUR) and the mean Gd-EOB-DTPA uptake rate (KI) of the whole liver correlated strongly with liver function and that there was a moderate correlation between RE and the MUR [30]. Geisel et al. also found that RE and the hepatic uptake index (HUI) correlate with MUR [31]. These studies suggested that the assessment of liver function with Gd-EOB-DTPA MRI is comparable with imaging with ^{99m}Tc -mebrofenin or GSA. Compared with signal intensity, quantitative parameters such as KI, T1 values and T2* values (obtained from T1 mapping [9] and T2* mapping [32], respectively) can reflect liver function more accurately, but the data acquisition obstacles and the uncertainty of the optimum pharmacokinetic model and most suitable parameters might limit their application. Nevertheless, these results indicate that GD-EOB-DTPA MRI will be an ideal choice for preoperative liver function evaluations.

Our study had several limitations. First, the severity of cirrhosis was not grouped based on liver biopsy results. Second, we did not classify the causes of cirrhosis, and the different causes might lead to different patterns of uptake and excretion of Gd-EOB-DTPA. Third, it was difficult to avoid selection bias because of the retrospective nature of this study. Fourth, this study included a small number of patients with Child–Pugh class C disease, who have a poor physical condition and decompensated cirrhosis and cannot undergo the examination; thus, further prospective and multicenter studies that include more patients with Child–Pugh class C disease are needed, and classify the causes of cirrhosis. Finally, this study only evaluated whole liver function. In clinical work, segmental liver function is more meaningful than whole liver function. Therefore, we will measure and explore segmental liver function according to liver segment in the future.

Conclusion

The liver function can be assessed and classified using LPC, LSC and the liver parenchyma SI obtained in the hepatobiliary phase with Gd-EOB-DTPA-enhanced MR imaging, the LPC might be a more useful imaging biomarker for the evaluation of liver function compared with LSC and the liver parenchyma SI. In addition, the portal vein SI in each group showed a certain increasing trend, it was unable to be used to reflect the liver function of patients with cirrhosis. But it is precisely because of the changing trend of portal vein signal that LPC can better reflect the liver function of patients with cirrhosis.

Abbreviations

Gd-EOB-DTPA: gadolinium-ethoxybenzyl-diethylenetriamine penta-acetic acid; MRI: magnetic resonance imaging; LPC: liver-to-portal vein contrast ratio; LSC: liver-to-spleen contrast ratio; PSC: portal vein-to-spleen contrast ratio; SI: signal intensity; AUC: area under curve; ROI: region-of-interest; HBP: hepatobiliary phase; MELD: model for end-stage liver disease; TB: total bilirubin; INR: international normalized ratio; PT: Prothrombin time; AST: aspartate transaminase; ALT: alanine transaminase.

Declarations

Acknowledgements

We gratefully acknowledge Professor Junkang Shen for providing valuable comments and suggestions for our paper. In addition, this work was supported in part by Suzhou Livelihood Technology – Project of Scientific Industry Demonstration [grant numbers: SS2019012].

Authors' contributions

MY and YZ proposed the method, analyzed data and wrote the manuscript. WZ and SG manually plotted all the ROIs, and participated in manuscript revisions, and provided critical review that helped in improving the manuscript. WC and HW collected clinical data and laboratory tests from all patients. All authors read and approved the final manuscript.

Funding

This study was funded by Suzhou Livelihood Technology – Project of Scientific Industry Demonstration [grant numbers: SS2019012].

Availability of data and materials

Data related to the current study are available from the corresponding author on reasonable request.

Competing interests

The authors declare that they have no competing interests.

Ethics approval and consent to participate

All procedures performed in studies involving human participants were in accordance with the ethical standards of the institutional and/or national research committee and with the 1964 Helsinki declaration and its later amendments or comparable ethical standards. For this type of study formal consent is not required.

Consent for publication

Not applicable.

References

1. Schuhmann-Giampieri G, Schmitt-Willich H, Press WR, Negishi C, Weinmann HJ, Speck U. Preclinical evaluation of Gd-EOB-DTPA as a contrast agent in MR imaging of the hepatobiliary system. *Radiology*. 1992;183(1):59-64.

2. Hinrichs H, Hinrichs JB, Gutberlet M, Lenzen H, Raatschen HJ, Wacker F, Ringe KI. Functional gadoxetate disodium-enhanced MRI in patients with primary sclerosing cholangitis (PSC). *Eur Radiol.* 2016;26(4):1116-24.
3. Purysko AS, Remer EM, Veniero JC. Focal liver lesion detection and characterization with GD-EOB-DTPA. *Clin Radiol.* 2011;66(7):673-84.
4. Kobayashi S, Matsui O, Gabata T, Koda W, Minami T, Ryu Y, Kozaka K, Kitao A. Relationship between signal intensity on hepatobiliary phase of gadolinium ethoxybenzyl diethylenetriaminepentaacetic acid (Gd-EOB-DTPA)-enhanced MR imaging and prognosis of borderline lesions of hepatocellular carcinoma. *Eur J Radiol.* 2012;81(11):3002-9.
5. Tsuboyama T, Onishi H, Kim T, Akita H, Hori M, Tatsumi M, Nakamoto A, Nagano H, Matsuura N, Wakasa K, Tomoda K. Hepatocellular carcinoma: hepatocyte-selective enhancement at gadoxetic acid-enhanced MR imaging—correlation with expression of sinusoidal and canalicular transporters and bile accumulation. *Radiology.* 2010;255(3):824-33.
6. Saito K, Moriyasu F, Sugimoto K, Nishio R, Saguchi T, Nagao T, Taira J, Akata S, Tokuyue K. Diagnostic efficacy of gadoxetic acid-enhanced MRI for hepatocellular carcinoma and dysplastic nodule. *World J Gastroenterol.* 2011;17(30):3503-9.
7. Noda Y, Goshima S, Kajita K, Kawada H, Kawai N, Koyasu H, Matsuo M, Bae KT. Biliary tract enhancement in gadoxetic acid-enhanced MRI correlates with liver function biomarkers. *Eur J Radiol.* 2016;85(11):2001-7.
8. Utsunomiya T, Shimada M, Hanaoka J, Kanamoto M, Ikemoto T, Morine Y, Imura S, Harada M. Possible utility of MRI using Gd-EOB-DTPA for estimating liver functional reserve. *J Gastroenterol.* 2012;47(4):470-6.
9. Katsube T, Okada M, Kumano S, Hori M, Imaoka I, Ishii K, Kudo M, Kitagaki H, Murakami T. Estimation of liver function using T1 mapping on Gd-EOB-DTPA-enhanced magnetic resonance imaging. *Invest Radiol.* 2011;46(4):277-83.
10. Chen BB, Hsu CY, Yu CW, Wei SY, Kao JH, Lee HS, Shih TT. Dynamic contrast-enhanced magnetic resonance imaging with Gd-EOB-DTPA for the evaluation of liver fibrosis in chronic hepatitis patients. *Eur Radiol.* 2012;22(1):171-80.
11. Esterson YB, Flusberg M, Oh S, Mazzariol F, Rozenblit AM, Chernyak V. Improved parenchymal liver enhancement with extended delay on Gd-EOB-DTPA-enhanced MRI in patients with parenchymal liver disease: associated clinical and imaging factors. *Clin Radiol.* 2015;70(7):723-9.
12. Motosugi U, Ichikawa T, Sou H, Sano K, Tominaga L, Kitamura T, Araki T. Liver parenchymal enhancement of hepatocyte-phase images in Gd-EOB-DTPA-enhanced MR imaging: which biological markers of the liver function affect the enhancement. *J Magn Reson Imaging.* 2009;30(5):1042-6.
13. Leinhard OD, Dahlström N, Kihlberg J, et al. Quantifying differences in hepatic uptake of the liver specific contrast agents Gd-EOB-DTPA and Gd-BOPTA: a pilot study. *Eur Radiol.* 2012;22(3):642-53.
14. Yoon JH, Lee JM, Kim E, Okuaki T, Han JK. Quantitative Liver Function Analysis: Volumetric T1 Mapping with Fast Multisection B1 Inhomogeneity Correction in Hepatocyte-specific Contrast-

- enhanced Liver MR Imaging. *Radiology*. 2017;282(2):408-417.
15. Lodge JPA. Assessment of hepatic reserve for the indication of hepatic resection: how I do it. *J Hepatobiliary Pancreat Surg*. 2005;12(1):4-9.
 16. van Montfoort JE, Stieger B, Meijer DK, Weinmann HJ, Meier PJ, Fattinger KE. Hepatic uptake of the magnetic resonance imaging contrast agent gadoxetate by the organic anion transporting polypeptide Oatp1. *J Pharmacol Exp Ther*. 1999;290(1):153-7.
 17. Weinmann HJ, Bauer H, Frenzel T, Mühler A, Ebert W. Mechanism of hepatic uptake of gadoxetate disodium. *Acad Radiol*. 1996; 3:S232-4.
 18. Beers BEV, Pastor CM, Hussain HK. Primovist, Eovist: What to expect. *J Hepatol*. 2012;57(2):421-9.
 19. Tamada T, Ito K, Sone T, Kanki A, Sato T, Higashi H. Gd-EOB-DTPA enhanced MR imaging: Evaluation of biliary and renal excretion in normal and cirrhotic livers. *Eur J Radiol*. 2011;80(3):e207-11.
 20. Verloh N, Utpatel K, Haimerl M, Zeman F, Fellner C, Fichtner-Feigl S, Teufel A, Stroszczyński C, Evert M, Wiggermann P. Liver fibrosis and Gd-EOB-DTPA-enhanced MRI: A histopathologic correlation. *Sci Rep*. 2015;5:15408.
 21. Kanki A, Tamada T, Higaki A, Noda Y, Tanimoto D, Sato T, Higashi H, Ito K. Hepatic parenchymal enhancement at Gd-EOB-DTPA-enhanced MR imaging: correlation with morphological grading of severity in cirrhosis and chronic hepatitis. *Magn Reson Imaging*. 2012;30(3):356-60.
 22. Zhang W, Wang X, Miao Y, Hu C, Zhao W. Liver function correlates with liver-to-portal vein contrast ratio during the hepatobiliary phase with Gd-EOB-DTPA-enhanced MR at 3 Tesla. *Abdom Radiol (NY)*. 2018;43(9):2262-9.
 23. Lee NK, Kim S, Kim GH, Heo J, Seo HI, Kim TU, Kang DH. Significance of the "Delayed hyperintense portal vein sign" in the hepatobiliary phase MRI obtained with Gd-EOB-DTPA. *J Magn Reson Imaging*. 2012;36(3):678-85.
 24. Kamisako T, Kobayashi Y, Takeuchi K, Ishihara T, Higuchi K, Tanaka Y, Gabazza EC, Adachi Y. Recent advances in bilirubin metabolism research: the molecular mechanism of hepatocyte bilirubin transport and its clinical relevance. *J Gastroenterol*. 2000;35(9):659-64.
 25. Takatsu Y, Kobayashi S, Miyati T, Shiozaki T. A novel method for evaluating enhancement using gadolinium-ethoxybenzyl-diethylenetriamine penta-acetic acid in the hepatobiliary phase of magnetic resonance imaging. *Clin Imaging*. 2016;40(6):1112-7.
 26. Kumazawa K, Edamoto Y, Yanase M, Nakayama T. Liver analysis using gadolinium-ethoxybenzyl-diethylenetriamine pentaacetic acid-enhanced magnetic resonance imaging: Correlation with histological grading and quantitative liver evaluation prior to hepatectomy. *Hepatol Res*. 2012;42(11):1081-8.
 27. Saito K, Ledsam J, Sourbron S, Hashimoto T, Araki Y, Akata S, Tokuyue K. Measuring hepatic functional reserve using low temporal resolution Gd-EOB-DTPA dynamic contrast-enhanced MRI: a preliminary study comparing galactosyl human serum albumin scintigraphy with indocyanine green retention. *Eur Radiol*. 2014;24(1):112-9.

28. Ho CM, Dhawan A, Hughes RD, Lehec SC, Puppi J, Philippeos C, Lee PH, Mity RR. Use of indocyanine green for functional assessment of human hepatocytes for transplantation. *Asian J Surg.* 2012;35(1):9-15.
29. Geisel D, Lüdemann L, Hamm B, Denecke T. Imaging-Based Liver Function Tests—Past, Present and Future. *Rofo.* 2015;187(10):863-71.
30. Rassam F, Zhang T, Cieslak KP, Lavini C, Stoker J, Bennink RJ, van Gulik TM, van Vliet LJ, Runge JH, Vos FM. Comparison between dynamic gadoxetate-enhanced MRI and 99mTc-mebrofenin hepatobiliary scintigraphy with SPECT for quantitative assessment of liver function. *Eur Radiol.* 2019;29(9):5063-72.
31. Geisel D, Lüdemann L, Fröling V, et al. Imaging-based evaluation of liver function: comparison of 99mTc-mebrofenin hepatobiliary scintigraphy and Gd-EOB-DTPA-enhanced MRI. *Eur Radiol.* 2015;25(5):1384-91.
32. Katsube T, Okada M, Kumano S, Imaoka I, Kagawa Y, Hori M, Ishii K, Tanigawa N, Imai Y, Kudo M, Murakami T. Estimation of liver function using T2* mapping on gadolinium ethoxybenzyl diethylenetriamine pentaacetic acid enhanced magnetic resonance imaging. *Eur J Radiol.* 2012;81(7):1460-4.

Figures

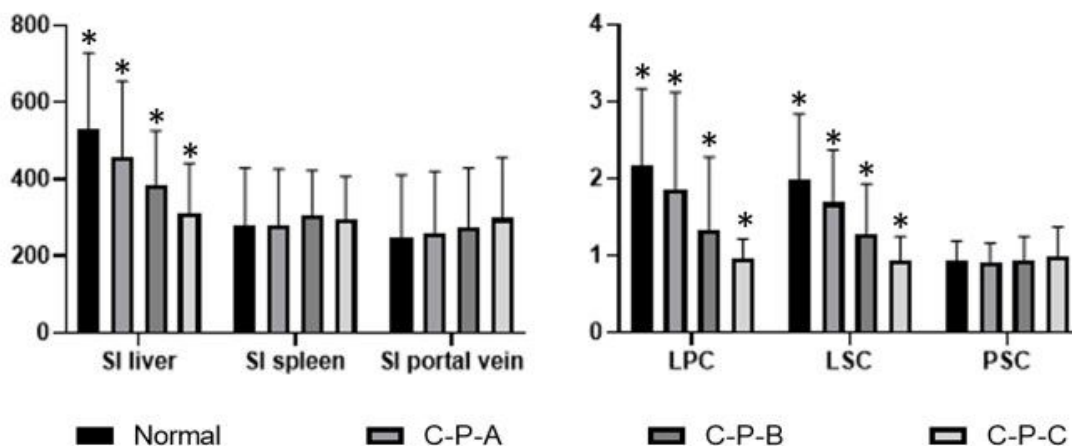


Figure 1

Differences in MRI data among groups on 15-min HBP images, data was presented as mean \pm 2SD, *there were statistical differences $p < 0.05$).

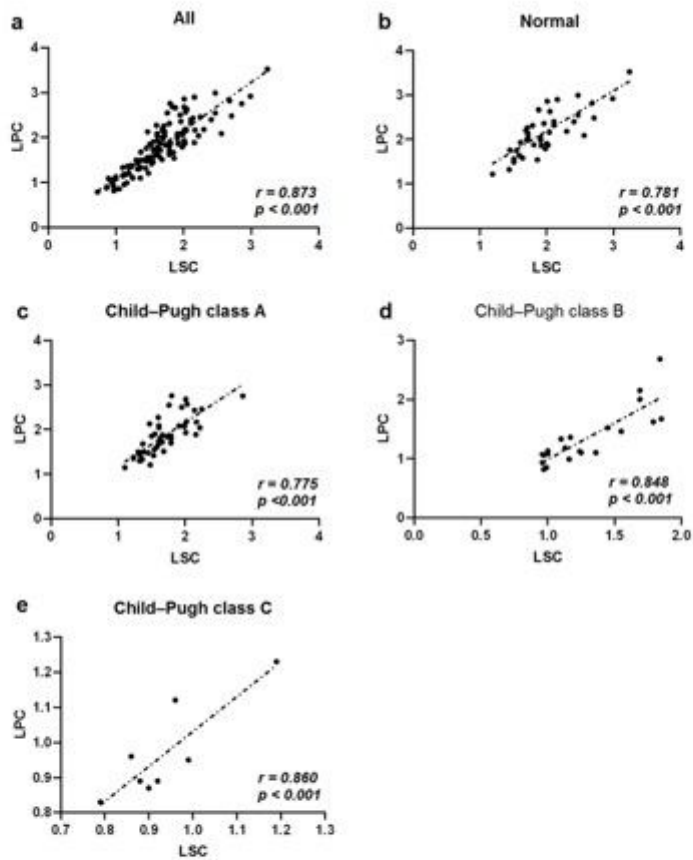


Figure 2

Correlations between LSC and LPC among the groups: (a) overall, (b) normal, (c) C-P A, (d) C-P B, and (e) C-P C. These correlations were strongly positive.

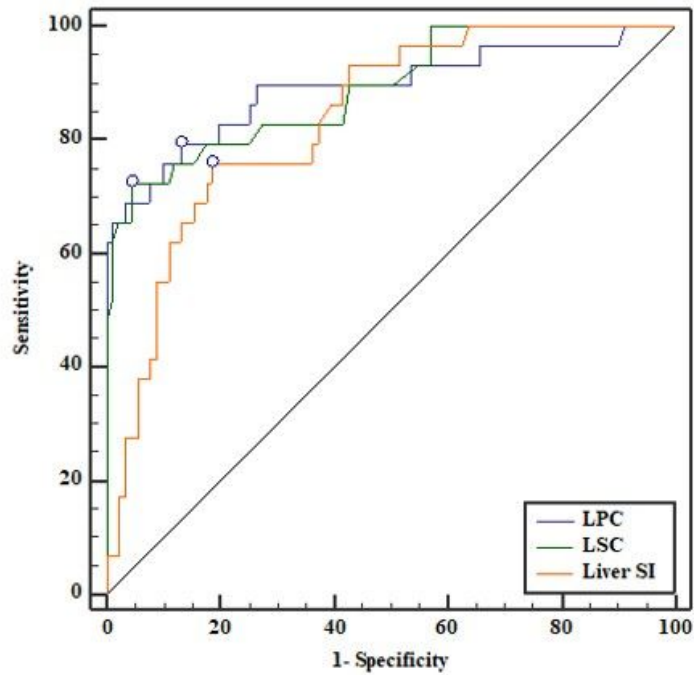


Figure 3

The ROC curve showed that the AUC value of LPC was 0.892 (95%CI 0.822 – 0.941), the AUC value of LSC was 0.889 (95%CI 0.818 – 0.939), and the AUC value of the liver parenchyma SI was 0.836 (95%CI 0.758 – 0.898).

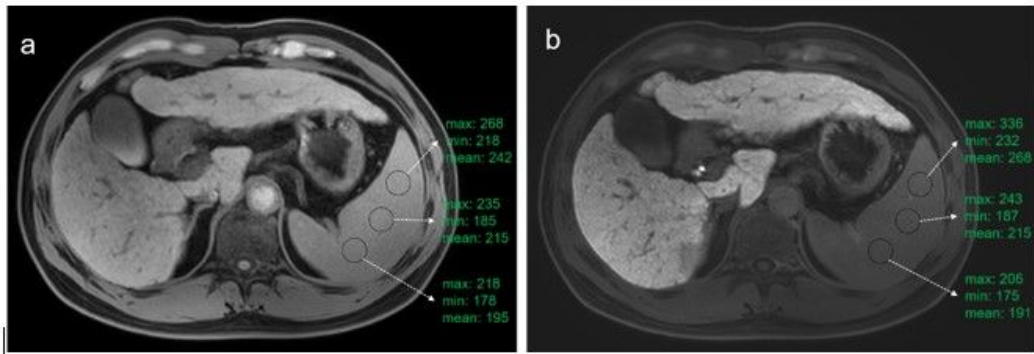


Figure 4

A case of liver cirrhosis with uneven spleen signal: (a) pre-enhanced image (b) hepatobiliary phase at 15 min image. ROI size: 200 mm × mm.

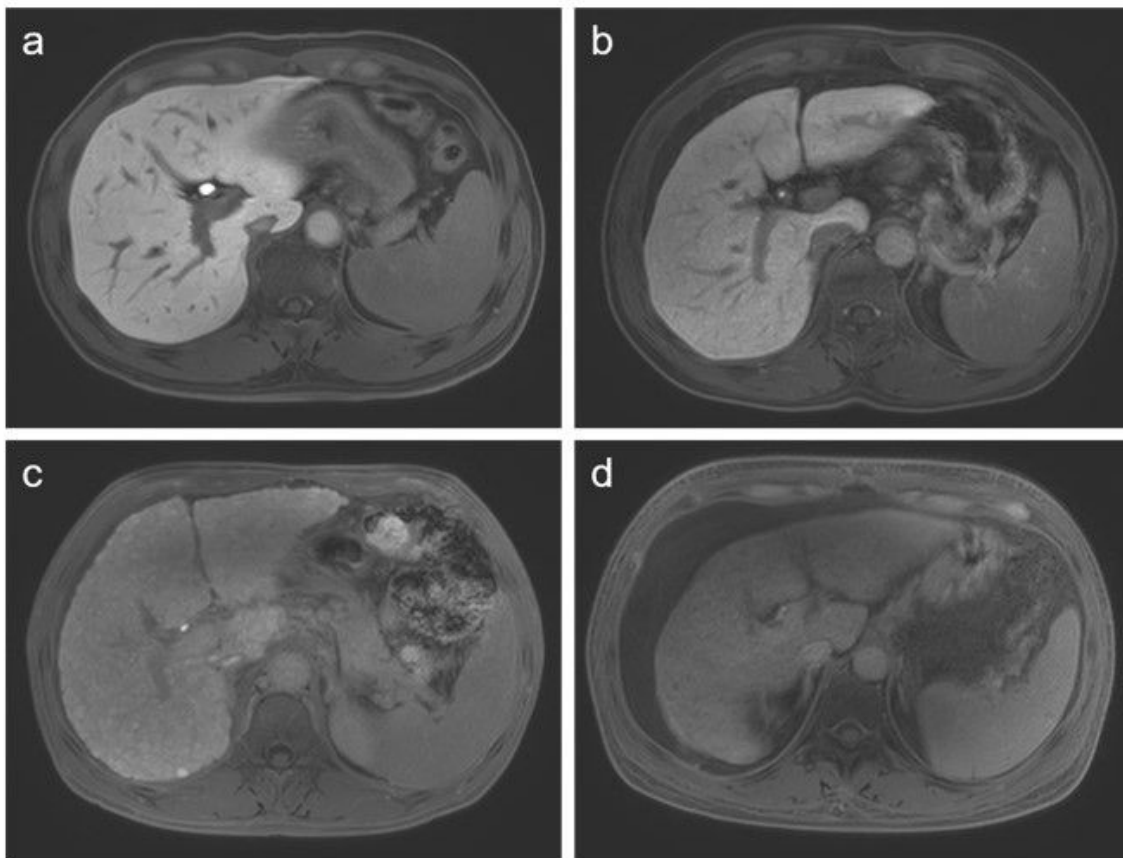


Figure 5

Hepatobiliary phase at 15 min images among the groups: (a) normal, (b) Child–Pugh A, (c) Child–Pugh B, (d) Child–Pugh C, the direct bilirubin of this patient was 2.38 mg/dl.